JOURNAL OF MATERIALS SCIENCE 32 (1997) 1741–1747

Ageing behaviour of SiC_p-reinforced AA 7075 composites

CHAI-YUAN SHEU, SU-JIEN LIN
Department of Materials Science and Engineering, National Tsing Hua University, Hsinchu, Taiwan

The precipitation behaviour in 7075 aluminium alloy matrix composites reinforced with 0–40 vol % particulate SiC_p (12.5 μm) was studied using macrohardness (HV) measurements and differential scanning calorimetry (DSC). In the low volume percentage (5, 10) SiC_p composites, the hardness–ageing curves and DSC scans are similar to those of the unreinforced alloy. However, the age-hardening quantities and DSC Gurnier-Preston (GP) zone peak size are smaller than those of the unreinforced alloy. Additionally, the high-temperature peaks (ageing curves at 200 °C or DSC scanning curves) are broader. In the high volume percentage (20, 30, 40) SiC_p composites, the hardness–ageing curves and DSC scans are very different from those of the unreinforced alloys. Only a high-temperature broad peak was observed during the DSC scanning. On the hardness–ageing curves no hardening phenomena were detected, but rather a softening phenomenon occurred in the 30% or 40% SiC_p composites, suggesting that during ageing an exothermic dislocation recovery softening process coexists with precipitation hardening. A model was introduced by dividing the matrix of the composite into Region I (normal precipitation) and Region II (particular precipitation). The precipitation of GP zones is completely suppressed and the precipitation of η′ phase is accelerated in Region II. The matrix of the low volume fraction SiC_p composite comprises Regions I and II, whereas that of the high volume fraction SiC_p composite comprises only Region II. The ageing behaviour and DSC scans of the composites can be fully explained by this model.

1. Introduction

Because the introduction of reinforcement can lead to a complicated strengthening response, a thorough investigation of the overall strength of metal matrix composites is difficult. Many different strengthening mechanisms in composites have been proposed by Christman *et al.* [1]. The development of matrix and interfacial microstructure in response to ageing treatments is included among them. An understanding of the ageing behaviour is, therefore, essential to a rigorous development of composite strengthening theories.

In a significant number of previous investigations, the presence of reinforcement was found significantly to affect the overall ageing behaviour of the matrix [2]. Accelerated ageing of the matrix is obtained in the composites rather than in the unreinforced materials subjected to an identical ageing treatment [2–14]. The relative amounts of the various precipitated phases are affected by the presence of reinforcement which, however, does not alter the precipitation sequences in the composites [6–9, 12], but significantly decreases the peak hardness achievable in the composite relative to the unreinforced matrix [12, 15–18].

The increased dislocation density introduced by quenching from the solution temperature due to the coefficient of thermal expansion (CTE) mismatch between the matrix and the reinforcement, affects precipitation [7, 12, 19, 20]. The absorption of quench-in vacancies in the high dislocation density matrix inhibits the Gurnier-Preston (GP) zone precipitation because nucleation requires vacancy clusters [15]. On the other hand, the high dislocation density can provide a rapid diffusion path, thus accelerating precipitation [6, 11–13, 21]. The role of the reinforcement in the precipitation kinetics is still ambiguous.

The aim of this work was to study the ageing behaviour of SiC_p-reinforced 7075 aluminium alloy over a wide range of volume per cent of carbide (0%–40%) and ageing temperatures (80–300 °C), and to clarify the effect of the reinforcement on precipitation in these composites.

2. Experimental procedure

An aluminium alloy, AA 7075, was reinforced with type 1200 (12.5 μm) SiC_p at various amounts (5, 10, 20, 30, 40 vol %). Gas-atomized 7075 aluminium alloy powder (44 μm) and SiC_p particulates were mixed and hot-pressed at 460 °C under a pressure of 200 MPa. The hot-pressed specimens were subsequently hot extruded to full density with a 9:1 reduction of area. The unreinforced material was

0022–2461

prepared under identical conditions. Chemical analysis of as-extruded specimens showed that the matrix alloy contained 5.5 wt% zinc, 1.6 wt% copper, 2.5 wt% magnesium, and 0.23 wt% iron.

The ageing behaviour was examined by macrohardness measurements, which were carried out using a Vickers hardness testing machine with an applied load of 20 kg and a loading time of 15 s. Specimens were prepared in the form of discs of 10 mm diameter, 5 mm thick, and were polished to a 6 μm finish. They were subsequently solution treated at 470 °C for an hour and quenched in water at room temperature. Artificial ageing was conducted in an oil bath at 80, 120 and 200 °C. Specimens were stored in liquid nitrogen prior to ageing and for any interim of the hardness measurement. At least five measurements were made for each ageing condition to ensure statistically valid results.

In order to investigate the effect of reinforcement on dislocation recovery, isothermal annealing treatment at 300 °C was also carried out after solution treatment and quenching.

For the differential scanning calorimetry (DSC) analyses, 1.6 mm thick, 5.5 mm diameter discs were prepared from the as-extruded material. These samples were solution treated at 470 °C for an hour and quenched in water at room temperature. They were stored in liquid nitrogen before DSC analysis. DSC scans were performed using DuPont 910 and 2100 thermal analysers with plug-in DSC modules. All of the DSC runs started at 25 °C and ended at 450 °C. A constant heating rate of 10 °C min^{-1} was used. Subsequently, the DSC data were converted to the differential heat capacity, ΔC_p, by using a calibration factor. The area of the peak in the DSC thermogram gives the matrix reaction enthalpy, which is related to the molar heat of reaction and the volume fraction of the precipitating or dissolving phase, while the peak temperature is related to the size and stability of the precipitate and to the reaction kinetics.

3. Results

Fig. 1 shows typical microstructures of the composites. The distribution of SiC particles is very uniform and no obvious microporosity can be observed. From density measurements, it was confirmed that the composites were fully densified. These data show that the hot pressing and extrusion process is a successful technique to fabricate the type 1200 SiC_p/7075 Al composites.

Fig. 2a shows the hardness curves for the unreinforced AA 7075 alloy and the composites aged at 120 °C. The hardness values at zero ageing time are those of as-quenched samples. These values are: HV 87, 94, 100, 115, 140 and 181, and correspond to 0, 5, 10, 20, 30, and 40 vol% SiC_p, respectively. It is clear that hardening becomes more effective with increasing volume percentage of SiC_p. For example, an increase in SiC_p content from 30 vol% to 40 vol% leads to an HV 41 increment, whereas increase from 10 vol% to 20 vol% leads to an HV 15 increment.

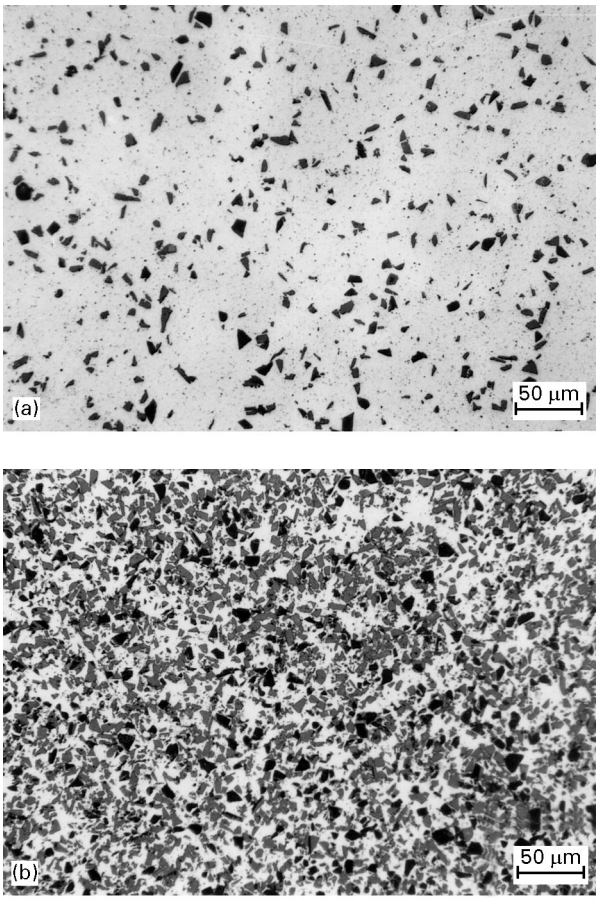

Figure 1 Photographs of type 1200 SiC_p/7075 Al composites containing (a) 5 vol% and (b) 40 vol% SiC_p.

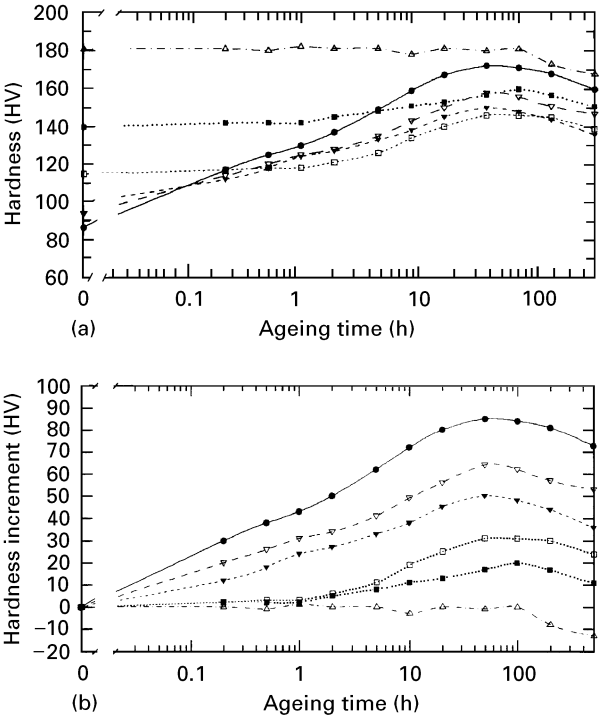

Figure 2 Hardness–ageing curves of type 1200 SiC_p/7075 Al composites containing various amounts of reinforcement (0–40 vol.%) and aged at 120 °C: (a) Hardness, (b) hardness increment: (●) 7075 Al, (▽) 5, (▼) 10, (□) 20, (■) 30, (△) 40 vol% SiC_p.

The hardness ageing curves shown in Fig. 2a indicate various ageing behaviours for different samples. For 7075 Al alloy the hardness rises from HV 81 to

HV 172. Composites containing up to 30 vol% SiC_p are softer than 7075 Al alloy after ageing. Fig. 2b is deduced from Fig. 2a by comparing the aged hardness to the as-quenched hardness for the same sample. It exhibits the hardness increment and shows the ageing behaviour of the specimen more clearly than Fig. 2a. Three characteristics can be identified. First, the 120 °C ageing hardness increments of the composites are always smaller than that of 7075 Al alloy, as previously reported [15, 16, 22, 23]. Second, as the reinforcement content increases, the age-hardening ability decreases. At the limit, the 40 vol% SiC_p composites did not exhibit any age-hardening. Ikeno *et al.* also reported no age-hardening for 20 vol% δ-Al_2O_{3sf}/Al–1% Mg_2Si [17] and Al_2O_{3p}/Al–4% Cu [18] composites. However, this phenomenon was not extensively reported. Third, the ageing kinetic seems no different between 7075 Al and some composites. For lower volume fraction composites (5, 10 vol%), the trend of the hardness–ageing curves is similar to that of 7075 Al alloy. The required time to reach maximum hardness remains almost the same.

It is well known that the precipitation sequence in 7075 Al alloy is: GP zone(s) → η' → η when the ageing temperature is below 190 °C [21, 24, 25]. In the two-stage ageing curve of 7075 Al alloy in Fig. 2b, the underaged hardening may be attributed to the GP zones and the peak-aged hardening to the η' phase [25–27]. Fig. 2b shows that with increasing carbide content, precipitation of GP zones is suppressed, but there is no effect on η' precipitation. However, these phenomena are still ambiguous. Hence, two ageing treatments were conducted: one at 80 °C in which case the major precipitates (at least in the underaged stage) are GP zones, and the other at 200 °C where η' and η phases precipitate [24].

Fig. 3 shows the hardness–ageing curves at 80 °C for the 7075 Al alloy and the composites. The ageing curve of the 7075 Al alloy indicates that the precipitation hardening may result from the GP zones during the initial ageing stage ($\leqslant$ 50 h). Reinforcement addition decreases the precipitation hardening effect of the GP zones. At or above 20 vol% SiC_p, the GP zone precipitation hardening is suppressed. The ageing curves of the 30 and 40 vol% SiC_p composites exhibit a minor softening trend which would indicate that some softening mechanism operates during ageing.

Fig. 4 shows similar curves for ageing at 200 °C. The hardening effect of the 7075 Al alloy resulted from the precipitation of η' phase [28]. The η phase precipitation has no strengthening effect [24]. Addition of reinforcement (5, 10 vol% SiC_p) broadens the hardening peak and reduces the time required to reach that peak. Thus it appears that the reinforcement addition accelerates the precipitation of η' phase. Similar results were previously reported [6, 7, 12]. However, the composite with 30 or 40 vol% SiC_p shows a softening phenomenon. These observations imply that a softening mechanism operates during ageing, and is more pronounced for higher volume fractions of SiC_p.

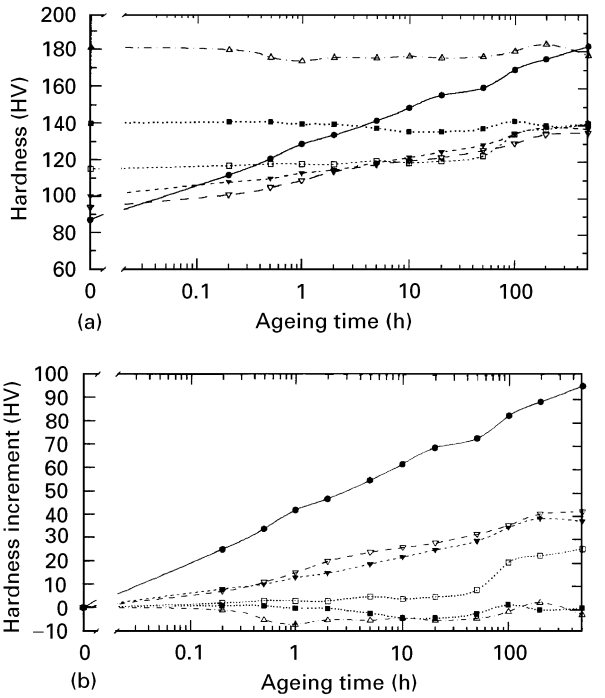

Figure 3 Hardness–ageing curves of type 1200 SiC_p/7075 Al composites containing various amounts of reinforcement (0–40 vol%) and aged at 80 °C: (a) Hardness, (b) hardness increment. For key, see Fig. 2.

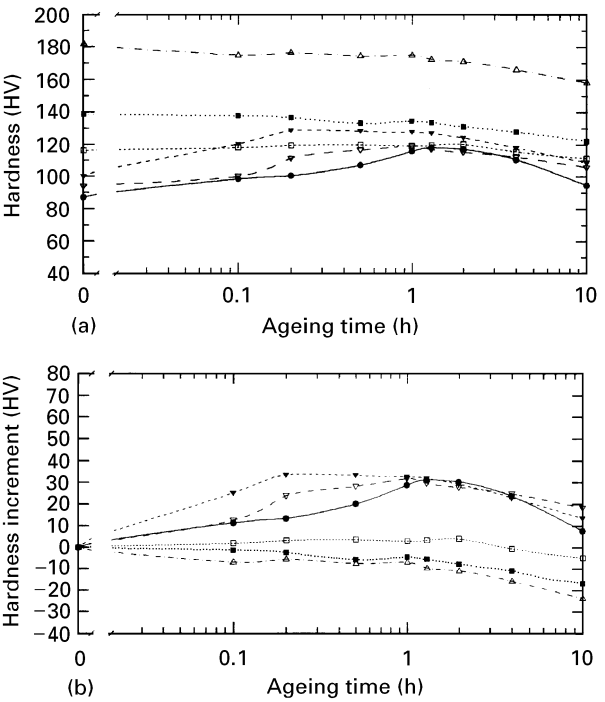

Figure 4 Hardness–ageing curves of type 1200 SiC_p/7075 Al composites containing various amounts of reinforcement (0–40 vol%) aged at 200 °C: (a) Hardness, (b) hardness increment. For key, see Fig. 2.

In order to explore further the softening mechanism, the as-quenched samples were heated to 300 °C for different times. Fig. 5 shows these annealing curves which suggest a set of dislocation recovery events. The hardness reduction or softening of the 40 vol% SiC_p composite after a 30 min annealing at 300 °C is HV 29 and for 7075 alloy it is just HV 4 for the same

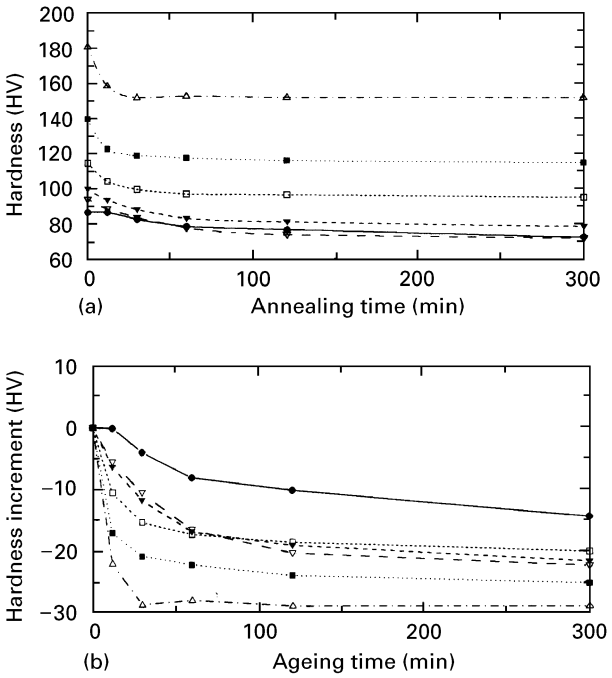

Figure 5 Softening phenomena of type 1200 SiC_p/7075 Al composites containing various amounts of reinforcement (0–40 vol%) annealed at 300 °C. (a) Hardness, (b) hardness increment. For key, see Fig. 2.

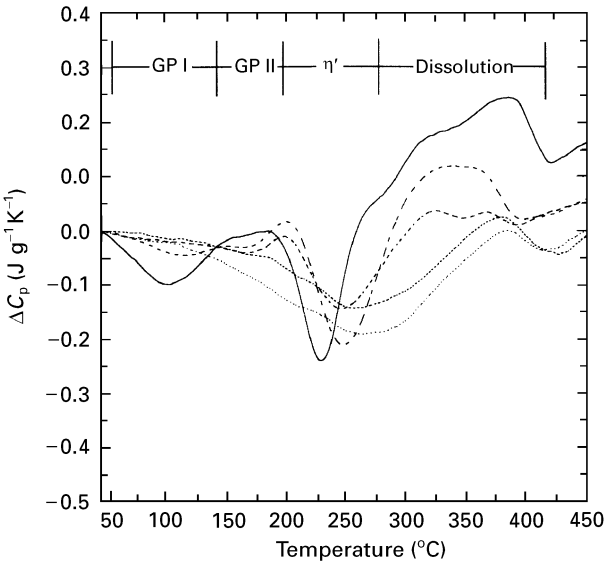

Figure 6 DSC thermogram of type 1200 SiC_p/7075 Al composites containing various amounts of reinforcement at a heating rate of 10 °C min^{-1}. (———) 7075 Al; SiC_p: (— — —) 5, (– – –) 10, (- - -) 20 and (· · ·) 40 vol%.

treatment. Because the measurement of hardness was conducted at room temperature, the softening value only reflects the thermal mismatch between SiC_p and the matrix during cooling from 470 °C to 300 °C, and can be larger than HV 30 for the higher volume fraction SiC_p composites. This value is sufficient to compensate the precipitation hardening of η′ phase, because the age hardening is also about HV 30 for the 7075 Al alloy aged at 200 °C.

Fig. 6 shows the DSC scans for the unreinforced 7075 Al alloy and its SiC_p composites. All of these specimens were in the as-quenched condition before DSC scanning. It is apparent that there are four distinct reaction regions for the 7075 Al alloy which can be characterized as follows [29–31]:

1. an exothermic peak between 45 and 150 °C, due to the formation of GP I zone;
2. an exothermic peak between 150 and 188 °C, due to the formation of GP II zone;
3. an exothermic peak between 188 and 266 °C, due to the formation of η′;
4. an endothermic peak between 266 and 420 °C, due to the dissolution of precipitates.

Fig. 6 indicates that the precipitation process of the low volume percentage (5, 10) SiC_p composites was similar to that of the unreinforced alloy; however, the precipitation peaks were shifted and their sizes varied. These phenomena are the same as those reported in SiC_p-reinforced 7475 Al [6] and SiC_p-reinforced 7091 Al [8] composites. The size of the GP zone formation peak in the composite was reduced, suggesting that the formation of these zones was significantly suppressed by the presence of the carbide. Furthermore, it is clear that the amount of GP zones formed in the composites decreased with increasing reinforcement content. Fig. 6 also shows the precipitation kinetics of GP zones was not accelerated by the presence of reinforcement and the temperature of the GP zone precipitation in composites did not change. This observation is contrary to the belief that the incubation time for the zone nucleation could be reduced because of the presence of high diffusivity paths in the composite matrix [3, 5, 7, 9, 11, 14, 21]. Furthermore, the hardness–ageing curves at 80 °C (Fig. 3) indicate the suppression of GP zones in the composites.

The DSC curves of the high volume fraction (20%, 40%) SiC_p composites are very different from that of the unreinforced 7075 Al alloy, exhibiting a broad reaction peak with no obvious separate GP zone peak. The precipitation sequence in these composites may have been altered and some additional exothermic reaction may have occurred in the composite matrix. In this case, the precipitation reaction peak would be superposed to the additional exothermic reaction peak during the DSC scan, leading to a broader peak. In addition, the total amount of exothermic enthalpy for the 40% SiC_p composite was larger than that for the 20% SiC_p composite, suggesting that the additional exothermic reaction became more extensive with increasing reinforcement content. This figure also shows that the maximum reaction rate of the broad peak occurred at about 270 °C, indicating that the additional exothermic reaction was dominant at the elevated temperatures. A comparison with the hardness results of the 300 °C annealing treatment suggests that the additional exothermic reaction may be the recovery softening of the composite matrix.

The above explanation shows that the η′ DSC peak in the low volume percentage (5, 10) SiC_p composites probably results from superposition of η′ phase precipitation and recovery reaction. Furthermore, the recovery process occurred at a higher temperature than that of η′ precipitation. Hence, the DSC η′ peak becomes broader and shifts to higher temperature, as shown in Fig. 6. Whether the η′ phase precipitation will be accelerated, does not follow from the DSC

data. However, the hardness–ageing curves of 200 °C indicate that the η′ precipitation is accelerated in the composites.

4. Discussion

The previous results clearly show that the introduction of carbide reinforcement considerably affects the overall ageing behaviour of 7075 aluminium alloy matrix, altering the amounts of various intermediate phases formed in the aluminium alloy matrix, and subsequently influencing the level of precipitation hardening. Also in the composites, recovery softening operates and is more significant at higher ageing temperatures in the high volume fraction SiC_p composites. The overall age-hardening behaviour of the composites can be attributed to a competition between precipitation hardening and recovery softening, both of which are related to the matrix dislocation density.

The distribution of the dislocations within the composite matrix is not uniform. The dislocation density is increased in a zone around the SiC_p reinforcement following quenching, due to the thermal expansion coefficient mismatch between the matrix and the reinforcement [19, 20]. Hence, the matrix in the composites could be divided into two regions, as shown schematically in Fig. 7, where Region I is the normal precipitation zone, far from the SiC_p/Al interface and Region II is the particular precipitation zone, near the SiC_p/Al interface. Because dislocation generation in Region I is not enough to alter the kinetics of the precipitation, the ageing behaviour therein is identical to that observed in the unreinforced alloy and is a normal precipitation hardening. The ageing response of Region II, on the other hand, is different because of the presence of a high dislocation density. These mass dislocations can be sinks for excess vacancies and channels for rapid diffusion paths. The high dislocation density in Region II could suppress a precipitation, such as GP zones, which need vacancy clusters as nucleation sites [15] and accelerate high-temperature precipitation which needs mass diffusion of solute atoms [3, 5, 6, 21]. Hence the particular precipitation of Region II could consist of a rapid η′ phase precipitation with no GP zone precipitation. Also, a high dislocation density means a high strain energy, thereby resulting in a high driving force for recovery. Thus Region II could simultaneously exhibit particular precipitation behaviour and recovery softening.

The relative volume fraction of Region II can alter the amounts of precipitates formed and the precipitation hardening potential, and subsequently strongly influence the overall ageing behaviour of the composites. The size of this region could depend on matrix yield strength, CTE (coefficient of thermal expansion) mismatch between matrix and reinforcement, solution temperature, quench rate, as well as reinforcement size, spacing and distribution [14]. In the present investigation, the volume fraction of Region II should only depend on and be proportional to the reinforcement concentration, increasing with it. The volume fraction of Region I, on the other hand, is significantly reduced with increasing reinforcement concentration.

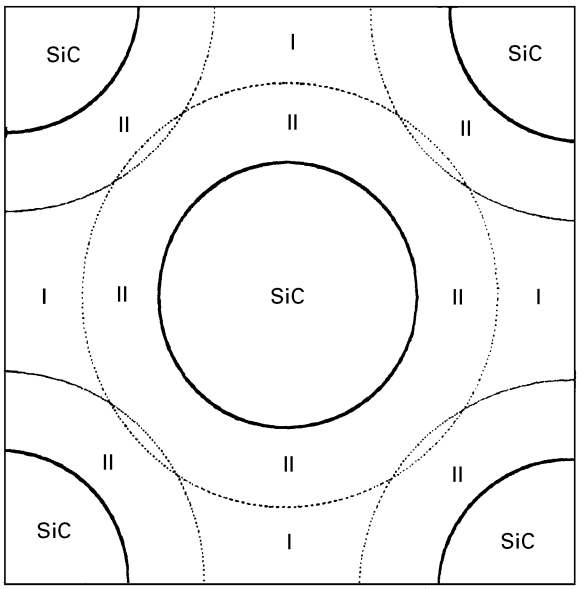

Figure 7 Schematic drawing of the normal precipitation, Region I, and the particular precipitation, Region II, in a composite. SiC_p particles are in a face centred cubic array and some overlapping of Region II is visible.

The knowledge of the size of Region II should contribute to the understanding of the mechanism of ageing behaviour in the composites. Several results obtained, such as the suppression of GP zones, could be used to predict the size of Region II. Results from ageing curves and DSC scans confirm that the GP zones were completely suppressed in the composites with 20 vol% SiC_p or more. The 20 vol% SiC_p composite has no obvious Region I, hence, Region II is very large. By assuming that the extent of Region II measured from the reinforcement centre is n multiplied by the SiC_p radius, R, the volume fraction of Region II, V_{II}, may be written for a spherical particle as

$$V_{II} = \left[\frac{(4/3)\pi(nR)^3}{(4/3)\pi R^3}\right] V_{SiC} - V_{SiC} \qquad (1)$$

where V_{SiC} is the volume fraction of SiC in the composite. The values of V_{II} for various reinforcement volume fractions obtained for different values of n, are summarized in Table I. Because the 20 vol% SiC_p composite no longer has GP zone precipitation, the volume fraction of Region I should be very small. For $n = 1.7$, the total volume fraction of Region II and SiC_p is 0.98 (from Equation 1) which is well above the close packing factor of face centred cubic array, 0.74. Hence, some overlapping of Region II exists. Subtracting the overlapping of Region II, the total volume fraction of Region II and SiC_p is 0.95. This means the volume fraction of Region I is only 0.05 and negligible. So thus it is reasonable to adopt $n = 1.7$.

From the above discussion, the thickness of Region II, $(n-1)R$, is about $0.7R$. This value is lower than that reported by Flom and Arsenault [19]. They reported the extent of the plastic zone that was $1.3R$ measured from the interface in the SiC/Al system. This difference is attributed primarily to the assumption that Region II, which can completely absorb the

TABLE I The volume fraction of Region II for the different values of n. Numbers in parentheses indicate the volume fraction of the reinforcement

	Volume fraction				
n	5% SiC_p	10% SiC_p	20% SiC_p	30% SiC_p	40% SiC_p
1.3	6% (11%)	12% (22%)	24% (44%)	36% (66%)	48% (88%)
1.4	9% (14%)	17% (27%)	34% (54%)	51% (81%)	68% (108%)
1.5	12% (17%)	24% (34%)	48% (68%)	72% (102%)	96% (136%)
1.6	16% (21%)	31% (41%)	62% (82%)	93% (123%)	124% (164%)
1.7	20% (25%)	39% (49%)	78% (98%)	117% (147%)	156% (196%)
1.8	24% (29%)	48% (58%)	96% (116%)	144% (174%)	192% (232%)

excess vacancies, has a rather higher dislocation density than that suggested by these authors [19]. Kim *et al.* [32] reported a dislocation density of 8.5×10^{13} m^{-2} at the interface, and decaying to a normal density of 5×10^{12} m^{-2}, at about $1.5R$ from the interface. The dislocation density at $0.7R$ from the interface is about 3.5 times the level of the background [32]. This indicates that high dislocation density is needed to change the precipitation kinetics.

Based on the above discussion, we can divide these composites into two kinds: low SiC_p (5, 10 vol%) and high SiC_p (20, 30, 40 vol%) composites. The matrix of the low SiC_p composites consists of a mixture of Regions I and II, whereas the matrix of the high SiC_p composites consists only of Region II. The ageing behaviour of the high SiC_p composites includes no GP zone precipitation, a faster η' phase precipitation, and recovery softening. For low-temperature ageing (80 °C), no GP zone precipitation occurs and no hardening phenomenon can be observed during the underaged period of the high SiC_p composite. In the 30 and 40 vol% SiC_p composites, Table I shows that Regions II substantially overlap, hence the dislocation density would be higher than that of the 20 vol% SiC_p composite. The driving force for dislocation recovery should also be higher than that in the 20 vol% SiC_p composites. Hence, some recovery softening can be seen in the ageing curves of the 30 and 40 vol% SiC_p composites aged at 80 °C, as shown in Fig. 3. For high-temperature ageing (200 °C), the hardening η' phase precipitation was accelerated and the recovery softening became more pronounced. These opposing processes compensated each other and no obvious age hardening was observed in the 20 vol% SiC_p composite. For the 30 or 40 vol% SiC_p composites, again, some softening has occurred owing to the more pronounced dislocation recovery during ageing. These phenomena can be observed in Fig. 4.

In the low SiC_p composite, the ageing behaviour resulted from the combination of Regions I and II, hence with coexistence of normal precipitation, particular precipitation, and recovery softening. However, recovery softening would have a minor effect because the volume fraction of Region II is low and there is no overlapping. For low-temperature ageing (80 °C), there exists partial GP zone precipitation hardening due to the presence of Region I, as shown in Fig. 3. For high-temperature ageing (200 °C), there exists an early η' phase precipitation hardening from Region II, and a normal η' phase precipitation hardening from Region I. Thus, a broad age-hardening peak, as shown in Fig. 4, was formed through combination of early and normal η' precipitations.

In the DSC scan curves (Fig. 6), the GP zone peak size was partially reduced because of the presence of some Region II and its peak temperature was the same as in the unreinforced alloy, due to the presence of Region I in the low SiC_p composites. In the high SiC_p composites (20, 30, 40 vol%), however, the GP zone exothermic peak was fully suppressed because the matrix was completely occupied by Region II. The high-temperature peak became broader with increasing volume fraction SiC_p. The reason is that the high-temperature peak is a combination of the η' peak and a higher temperature recovery peak. Increasing the volume fraction makes the recovery reaction more pronounced, leading to the higher temperature shift and broadening phenomenon of the peak.

5. Conclusions

1. In the low volume percentage (5, 10) SiC_p composites based on AA 7075 alloy, (a) the hardness–ageing curves and DSC scans are similar to those of the unreinforced alloy, (b) the age-hardening quantities and DSC GP zone peak size are smaller than those of the unreinforced alloy, and (c) the temperature peaks on the ageing curves at 200 °C or the DSC curves are always broader.

2. In the high volume percentage (20, 30, 40) SiC_p composites, (a) the hardness–ageing curves and DSC scans are very different from those of the unreinforced alloy, (b) only a high-temperature broad peak can be seen during DSC scanning, and (c) the hardness–ageing curves exhibit no hardening phenomena, but rather a softening phenomenon for the 30% or 40% SiC_p composites, suggesting that an additional exothermic process coexists with the precipitation.

3. A model was introduced by dividing the matrix of the composite into a region of normal precipitation and a region of particular precipitation. The ageing behaviour and DSC scans of the composites can be fully explained by this model.

Acknowledgements

The authors thank Professor Theo Z. Kattamis (visiting Professor at MIT) for his critical correction of the

English of the manuscript and many constructive suggestions. They also acknowledge the financial support provided by the National Science Council of Taiwan under Grant NSC-842216E007-026.

References

1. T. CHRISTMAN, A. NEEDLEMAN and S. SURESH, *Acta Metall.* **37** (1989) 3029.
2. T. G. NIEH and R. F. KARLAK, *Scripta Metall.* **18** (1984) 25.
3. J. CHRISTMAN, A. NEEDLEMAN, S. NUTT and S. SURESH, *Mater. Sci. Eng.* **A107** (1989) 49.
4. I. DUTTA and D. L. BOURELL, *ibid.* **A112** (1989) 67.
5. T. CHRISTMAN and S. SURESH, *Acta Metall.* **36** (1988) 1691.
6. J. M. PAPAZIAN, *Metall. Trans.* **19A** (1988) 2945.
7. I. DUTTA, S. M. ALLEN and J. L. HAFLEY, *ibid.* **22A** (1991) 2553.
8. J. L. PETTY-GALIS and R. D. GOOLSBY, *J. Mater. Sci.* **24** (1989) 1439.
9. C. BADINI, F. MARINO and A. TOMASI, *ibid.* **26** (1991) 6279.
10. M. J. HADIANFARD, YIU-WING MAI and J. C. HEALY, *ibid.* **28** (1993) 3665.
11. Y. SONG and T. N. BAKER, *Mater. Sci. Technol.* **10** (1994) 406.
12. I. DUTTA, C. P. HARPER and G. DUTTA, *Metall. Trans.* **25A** (1994) 1591.
13. L. SALVO and M. SUERY, *Mater. Sci. Eng.* **A117** (1994) 19.
14. I. DUTTA and D. L. BOURELL, *Acta Metall.* **38** (1990) 2041.
15. C. M. FRIEND and S. D. LUXTON, *J. Mater. Sci.* **23** (1988) 3173.
16. T. S. KIM, T. H. KIM, K. H. OH and H. I. LEE, *ibid.* **27** (1992) 2599.
17. S. IKENO, K. KAWASHIMA, K. MATSUDA, H. ANADA and S. TADA, *Keikinzoku Jpn* **40** (1990) 501.
18. *Idem*, *ibid.* **41** (1991) 752.
19. Y. FLOM and R. J. ARSENAULT, *Mater. Sci. Eng.* **75** (1985) 151.
20. R. J. ARSENAULT and N. SHI, *ibid.* **81** (1986) 175.
21. G. THOMAS and J. NUTTING, *J. Inst. Metals* **88** (1959–60) 81.
22. M. P. THOMAS and J. E. KING, *J. Mater. Sci.* **29** (1994) 5272.
23. E. HUNT, P. D. PITCHER and P. J. GREGSON, *Scripta. Metall.* **24** (1990) 937.
24. JOHN E. HATCH (ed.), "Aluminum: Properties and Physical Metallurgy" (ASM, Metals Park, OH, 1984).
25. J. K. PARK and A. J. ARDELL, *Metall. Trans.* **14A** (1983) 1957.
26. *Idem*, *Scripta. Metall.* **22** (1988) 1115.
27. J. LENDVAI, GY. HONYEK, and I. KOVACS, *ibid.* **13** (1979) 593.
28. I. J. POLMEAR, *J. Inst. Metals* **86** (1957–58) 535.
29. W. LACOM, H. P. DEGISCHER and C. Y. ZAHRA, *Scripta Metall.* **14** (1980) 253.
30. J. M. PAPAZIAN, *Metall. Trans.* **13A** (1982) 761.
31. D. J. LLOYD and M. C. CHATURVEDI, *J. Mater. Sci.* 17 (1982) 1819.
32. K. T. KIM, J. K. LEE and M. R. PLICHTA, *Metall. Trans.* **21A** (1990) 673.

Received 5 March
and accepted 3 October 1996